STEM CELLS AND DEVELOPMENT
Volume 22, Number 2, 2013

DOI: 10.1089/scd.2012.0220

Pkb/Akt1 Mediates Wnt/GSK3β/β-Catenin Signaling-Induced Apoptosis in Human Cord Blood Stem Cells Exposed to Organophosphate Pesticide Monocrotophos

Mahendra P. Kashyap,[1] Abhishek K. Singh,[1] Vivek Kumar,[1] Dharmendra K. Yadav,[2] Feroz Khan,[2] Sadaf Jahan,[1] Vinay K. Khanna,[1] Sanjay Yadav,[1] and Aditya B. Pant[1]

Inhibition mechanisms of protein kinase B (Pkb)/Akt and its consequences on related cell signaling were investigated in human umbilical cord blood stem cells (hUCBSCs) exposed to monocrotophos (MCP, an organophosphate pesticide). In silico data reveal that MCP interacts with kinase and c-terminal regulatory domains of Akt1, resulting into a total docking score of 5.2748 and also forms H-bond between its N-H and Thr-291 residue of Akt1, in addition to possessing several hydrophobic interactions. The main cause of Akt inhibition is considered to be the strong hydrogen bond between N-H and Thr-291, and hydrophobic interactions at Glu-234, and Asp-292 in the vicinity, which is usually occupied by the ribose of ATP, and interaction with residue Phe-161, thus leading to a significant conformational change in that particular portion of the protein. In silico data on Akt inhibition were confirmed by examining the downregulation of phosphorylated (Thr308/Ser493) Akt1 in MCP-exposed hUCBSCs. MCP-mediated altered levels of pAkt downstream targets viz., downregulated pGSK3β (Ser9), unchanged GSK3αβ, and upregulated levels of Bad, P^{53}, and caspase-9 further confirm the inhibition of pAkt. The cellular fate of such pAkt inhibition was confirmed by increased terminal deoxynucleotide transferase dUTP nick-end labeling positive cells, reduced mitochondrial membrane potential, and the activation of various MAPKs, proapoptotic markers-Bax, and caspases-9/3. Our data demonstrate that Akt1 plays a key role in MCP-induced apoptosis in hUCBSCs. We also identified that such cellular responses of human cord blood stem cells against MCP were due to strong binding and inhibition of kinase and AGC-Kinase-C terminal regulatory domains of Akt1.

Introduction

Protein kinase B (Pkb)/Akt, a serine/threonine-specific kinase, has a role in the regulation of multiple cellular processes that includes cell survival, cell proliferation, apoptosis, and glucose metabolism [1–3]. Akt regulates the cell survival pathways (IGF-1R/PI3K/PTEN/mTOR) and apoptosis suppression by inhibiting the proteins involved in cell death viz., ASK1/caspase-9/Bad/P^{53} and P^{21} [4]. It was discovered as a fusion protein in oncogenic retrovirus (AKR mouse thymoma), and found overexpressed in various types of cancers [5,6]. Three Akt genes exist in humans: *AKT1*, *AKT2*, and *AKT3*. *AKT1* has role in cell proliferation and growth [5], whereas *AKT2* is responsible for regulation of insulin-signaling pathway and required to induce glucose transport [7]. The exact role of *AKT*3 has not yet been defined; however, impaired brain development in mice and inhibition of N-cadherin-mediated cell motility in PyMT-N-cadherin cells have been reported due to lack of the *AKT3* gene and overexpression of the *AKT3* gene [8,9]. Akt possesses 3 domains viz., Pleckstrin Homology (PH) domain, kinase domain, and AGC-kinase C-terminal regulatory domain. The PH domain binds to either phosphatidylinositol-3, 4, 5,-trisphosphate (PIP3) or phosphatidylinositol-3,4-bisphosphate (PIP2). Once correctly bound to PIP3, Akt can then be phosphorylated at the kinase domain and the AGC-kinase C-terminal regulatory domain with the help of phosphoinositide-dependent kinase 1 (PDPK1, which phosphorylates at threonine 308) and mammalian target of rapamycin complex 2 (mTORC2, which phosphorylates at serine 473). In general, mTORC2 acts as PDK2 molecule; however, other molecules viz., DNA-PK, integrin-linked kinase, and PKCbII, have also been reported to phosphorylate Pkb Ser473, and thus serves as PDK2 in some cell types [4,10].

Phosphoinositide 3-kinase (PI3K) is the only enzyme that can phosphorylate PPI2 to PPI3, which eventually activates the cellular signaling in terms of cell proliferation and growth by means of activation of Akt1. In experimental conditions, the overexpression of a tumor suppressor (PTEN) was found to reverse this process by dephosphorylating PPI3 to PPI2 [4,11]. Akt also prevents the degradation of cyclin D1 by phosphorylating and

[1]In Vitro Toxicology Laboratory, Indian Institute of Toxicology Research, Council of Scientific & Industrial Research, Lucknow, India.
[2]Central Institute of Aromatic and Medicinal Plant, Council of Scientific & Industrial Research, Lucknow, India.

inhibiting GSK3β, attenuates the cell cycle inhibitors such as p21waf1 and p27kip1 by phosphorylating these proteins, and also phosphorylates BAD, which triggers its release from Bcl-2/Bcl-xL proteins in the mitochondrial membrane as well as procaspase 9, and thus helps in preventing the apoptosis [4].

Multiple efforts have been made to discover small-molecule antagonists that may hamper the different functions of Akt1 domains or their interacting proteins, since Akt inhibition considered an effective therapy against different types of cancer [5,12–16]. Some pesticides such as dieldrin and endosulfan induced ERβ-mediated activation of Akt phosphorylation in cortical neurons; however, in cerebellar granule cells, same dieldrin induced Akt Phosphorylation by multiple activation of ERα, ERβ, and G protein-coupled receptor 30. Thus, the extracts of these dieldrin- and endosulfan-treated cortical neurons induce the proliferative potential of cancerous MCF-7 cells [3]. Other reports indicate that the pesticide has role in inducing cell injuries by inhibiting pAkt that could result into hampered glucose metabolism in 3T3-L1 adipocytes [2]. Primarily, the Akt-mediated pathways have been explored in cancer to investigate the mechanisms of protection [5,13,15,16], but the mechanisms of Akt inhibition in noncancerous normal human stem cells are still to be explored. Thus, the present investigations were aimed to study the effect of the pesticide monocrotophos (MCP) on the activation of Akt/Pkb and their consequences on downstream signaling pathways in human umbilical cord blood stem cells (hUCBSCs). The reason for carrying out such types of studies in hUCBSCs is that because transplacental diffusion of pesticides and subsequent impaired hematopoiesis/and related disorders are well documented [17,18]; however, the underlying cell death mechanisms involved in hematopoietic stem cells are largely unknown. These cells are pluripotent in nature and give rise to all kind of hematopoietic and matrix cells in the organisms, and small injuries in these cells result into long-lasting consequences. The present investigation was carried out using an organophosphate pesticide, since the pesticide exposure in mice has already been reported to reduce the total number of bone marrow cells by arresting the hematopoietic and non-hematopoietic progenitor cells either in the G0/G1-phase or in the S/G2/M-phase, and subsequently impaired the hematological parameters. The results clearly indicated the significant long-lasting toxic effect of pesticides on the bone marrow microenvironment, which ultimately leads to the formation of a degenerative disease like aplastic anemia [19]. In the independent studies on infant acute and childhood leukemia, it has been reported that frequent exposure of insecticides during the gestation period and early stage of life poses significantly a higher risk of disease than later exposures. The hematotoxicological consequences through transplacental diffusion of pesticides were found to be greater than outdoor exposures of pesticides [20,21]. In the present investigations, MCP was selected as a model pesticide, as it is being used extensively worldwide for more than forty years, and its adverse outcomes have reported earlier by us [22,23].

Materials and Methods

In silico studies

Molecular modeling parameters and energy minimization. The molecular modeling of compounds viz., MCP and camptothecin, was performed with Protein kinase B (Pkb/Akt), a serine/threonine kinase, which plays a key role in the regulation of cell survival and proliferation, by using Sybyl X 1.3 molecular modeling and drug discovery software (www.tripos.com; SYBYL-X 1.3; Tripos International). All the molecules were initially designed in Sybyl, whereas the molecular construction, geometry optimization, and energy minimization process were performed using HP XW4600 workstation with Intel Core 2 Duo E8400 (3.2 GHz) processor and 4 GB of RAM, running the Red Hat® Enterprise Linux 4.0 (32-bit compatible) operating system (Silicon Graphics, Inc.). The Tripos force field with a distance-dependent dielectric and Powell gradient algorithm with a convergence criterion of 0.001 kcal mol^{-1} was used for optimization. Partial atomic charges were assessed using the Gasteiger-Hückel method. Two-dimensional structures were converted to three-dimensional structures using the program Concord v4.0, and the maximum number of iterations performed in the minimization was set to 2000. Further geometry optimization was done through the MOPAC-6 package using the semiempirical PM3 Hamiltonian method [24].

Molecular docking studies. To find out the possible bioactive conformations of different Akt inhibitors, the Sybyl X 1.3 interfaced with Surflex-Dock program [25] was operated to dock all the compounds into the active site of the Akt kianse (PDB code: 3CQU). The program automatically docks ligand into the binding pocket of an enzyme/receptor protein using a protomol-based algorithm and empirically produced scoring function. The protomol is a very important and necessary factor for docking algorithm and works as a computational representation of the proposed ligand that interacts into the binding site. Surflex-Dock's scoring function has several factors that play an important role in the ligand–receptor interaction, in terms of hydrophobic, polar, repulsive, entropic, and solvation, and it is a well-established and recognized method [26]. The most standard docking protocols have ligand flexibility into the docking process, while count the protein as a rigid structure [27]. Our molecular docking involves the following several steps: (1) the protein structure was imported into Surflex, and then hydrogens were added; (2) generation of protomol using a ligand-based strategy, and during this process, 2 parameters (first called protomol_bloat, which determines how far the site should extend from a potential ligand; and another called protomol_threshold, which determines deepness of the atomic probes that is used to define the protomol penetration into the protein) must be specified to form the appropriate binding pocket. Thus, in the current study, protomol_bloat was set to 0, and protomol_threshold was set to 0.50, when a reasonable binding pocket was obtained; and (3) all of the compounds were docked into the binding pocket, and 20 possible active docking conformations with different scores were obtained for each compound. During the docking process, all of the other parameters were assigned to their default values. Surflex-Dock total scores, which express the $-\log_{10}$ (Kd) units to represent binding affinities, were applied to estimate the ligand–receptor interactions of the newly designed molecules.

In vitro validation studies

Reagents and consumables. All the chemicals, reagents, and kits used in this study were purchased from Stem Cell Technologies and Sigma, unless otherwise stated. All

cytokines and growth factors such as recombinant human basic fibroblast growth factor (rhbFGF), thrombopoietin (rhTPO), stem cell factor (rhSCF), and fetal liver tyrosine kinase 3 ligand (rhFLT-3 Ligand) were purchased from PeproTech. All the antibodies were procured from Chemicon International and Abcam. Culture wares and plastic wares were procured from Nunc and Corning Incorporated. Autoclaved Milli-Q water was used in all the experiments.

Ethics clearance for collection and transportation of human tissues. The entire study was carried out by following the protocols and procedures approved by the Institutional Human Ethics Committees of Indian Institute of Toxicology Research (IITR), Lucknow, India, and the CSM Medical University, Lucknow, India. The informed consent of parents was obtained before collecting blood from umbilical cord.

Isolation and purification of human umbilical cord blood hematopoietic stem cells. The entire study was carried out by following the protocols and procedures approved by the Institutional Human Ethics Committees of the IITR, Lucknow, India, and the CSM Medical University, Lucknow, India. The informed consent of parents was received before collection of the blood from umbilical cord. Mothers enrolled in the study were of age range 24.5 ± 6.2 years. They fulfilled the entire inclusion criteria and were nonobese and free from malignancy or any other systemic disorder. Totally, 52 blood samples ($\sim$40 mL/cord) were collected from the cord vein in a sterile container having an anticoagulant citrate dextrose buffer and immediately transported to the IITR, Lucknow, for further processing. Blood was diluted in the ratio of 1:1 with Dulbecco's phosphate-buffered saline (DPBS) without Ca^{2+} and Mg^{2+}, pH 7.5 (Stem Cell Technologies). Subsequently, cord blood mononuclear cells were segregated through negative immunodepletion of $CD3^+$, $CD14^+$, $CD19^+$, $CD38^+$, and $CD66b^+$ cells using a RosseteSep™ cord blood CD34 Pre-enrichment Cocktail (Stem Cell Technologies; Catalog No. 15631C), according to the instructions given by the manufacturer, followed by Ficollpaque™ (1.077 g/cm^3; Stem Cell Technologies) density-gradient centrifugation (700 *g* for 30 min). $CD34^+$ hematopoietic stem cells were isolated from mononuclear cells using the automated robotic and magnetic cell separator RoboSep™ (Stem Cell Technologies; Catalog No. 20000) and an EasySep™ human cord blood CD34-positive selection kit (Stem Cell Technologies; Catalog No. 18056) possessing monoclonal bispecific antibodies against the human antigen CD34 and iron-core dextran-coated nanoparticles as per instructions from the manufacturer.

Proliferation and bulk production of hematopoietic stem cells. Freshly isolated hematopoietic stem cells were cultured in a plastic 25-cm^2 ultralow-attachment culture flask (Corning Incorporated) at a density of 1×10^5 cells/mL in 5 mL of a serum-containing medium, the myelocult medium (Stem Cell Technologies; Catalog No. H5150) supplemented with hydrocortisone (10^{-6} M) and other growth factors viz., rhbFGF (50 ng/mL), rhSCF (25 ng/mL), rhTPO (25 ng/mL), rhFLT-3 Ligand (10 ng/mL; PeproTech). Cells were maintained as suspension in a humidified atmosphere at 37°C and 5% CO_2. Half of the medium was changed twice in a week. At each passage, cells were checked for the $CD34^+$ marker to ascertain the purity of stem cells. Cells were subcultured at the confluence of 80%–90% in a myelocult medium supplemented with hydrocortisone and growth factor cocktails as earlier.

Purity analysis of stem cells. Enriched stem cells were analyzed for purity by quantifying the hematopoietic stem cell ($CD34^+$) and primitive stem cell ($Thy1^+$) markers. In brief, stem cells (1×10^5) were centrifuged at 200 *g* for 10 min and then stained with PE-Texas Red conjugated anti-CD34 and anti-Thy1 antibodies (Stem Cell Technologies) for 30 min at 4°C. The cells were then washed with DPBS and analyzed using flow cytometry (BD-FACS Canto) equipped with BD FACS Diva, version 6.1.2 software. The data are presented in percent population of stem cells.

Dose selection of MCP. Noncytotoxic doses of MCP used in the study were identified using standard endpoints of cytotoxicity, that is, 3-(4,5-dimethylthiazol-2-yl)-2,5-diphenyltetrazoliumbromide (MTT) and lactate dehydrogenase (LDH)-release assays.

MTT assay. The MTT assay was carried out as per the protocols described by us earlier [22]. In brief, stem cells (1×10^4 cells/well) were seeded in laminin- (25 μg/mL) precoated 96-well tissue culture plates (Corning Incorporated) and incubated under a high-humid environment in 5% CO_2 for 24 h at 37°C. After that, the medium was replaced with a fresh medium containing different concentrations of MCP (10^{-3} to 10^{-8} M). The cells were reincubated for 12–96 h, and thereafter the MTT assay was done. Tetrazolium bromide salt (10 μL/well; 5 mg/mL of stock in PBS) was added 4 h before the completion of respective incubation periods. Then, the reaction mixture was carefully taken out, and 200 μL of culture-grade DMSO was added to each well by pipetting up and down several times until the content gets homogenized. After 10 min, the color was read at 550 nm using a Multiwell Microplate Reader (Synergy HT; Bio-Tek). Parallel sets without MCP were also run under identical conditions that served as basal controls.

LDH assay. LDH release is a method to measure the membrane integrity as a function of the amount of cytoplasmic LDH released into the medium. The LDH assay was carried out using the readymade commercially available LDH assay kit for in vitro cytotoxicity evaluation (TOX-7; Sigma). The assay was based on the measurement of the activity of LDH release from damaged cells. The resulting colored compound was measured after the deduction of background at 690 nm using a Multiwell Microplate Reader (Synergy HT; Bio-Tek) at 490 nm. The culture conditions and MCP exposure and incubation periods were similar to that in MTT assay. After the respective exposure period (12–96 h), cells were removed from the CO_2 incubator and centrifuged at 250 *g* for 4 min. Then, the supernatant from each well was transferred to a fresh flat-bottom 96-well culture plates and processed for an enzymatic assay following the instructions and guidelines provided with the kit. A noncytotoxic dose (10^{-5} M) of MCP was used to study the alterations in the expression (mRNA and protein) of markers of apoptosis and cell death.

Oxidative stress

Reactive species generation. Estimation of MCP-induced reactive oxygen species (ROS) generation was carried out following the protocol described earlier by us [23]. In brief, cells (2×10^4 per well) were seeded in laminin- (25 μg/mL) precoated 96-well black-bottom culture plates and allowed to adhere for 24 h in 5% CO_2–95% atmosphere at 37°C. Thereafter, the medium was aspirated, and cells were exposed to

MCP (10^{-5} M), camptothecin (3 μg/mL), NAC (10 μM) and NAC + MCP (10 μM) for 6 h. After the exposure, cells were reincubated with 2′, 7′ dichlorodihydrofluorescein–diacetate (DCFH-DA) (20 μM) for 30 min at 37°C. Thereafter, the reaction mixture was replaced by PBS (200 μL per well). The plates were then kept on a rocker shaker platform for 10 min at room temperature in dark, and the fluorescence intensity was measured using a Multiwell Microplate Reader (Synergy HT; Bio-Tek) on excitation wavelength at 485 nm and emission wavelength at 528 nm. The data are expressed in percent of the unexposed control.

Estimation of intracellular glutathione levels. Glutathione (GSH) levels were assessed in the cells exposed to MCP (10^{-5} M), camptothecin (3 μg/mL), NAC (10 μM), and NAC + MCP (10 μM) for 6 h using a commercially available kit (Glutathione Detection Kit, Catalog No. APT250; Chemicon). In brief, after respective exposures, cells were collected through centrifugation at 700 *g* for 2 min at 4°C and lyzed in a lysis buffer. The samples were recentrifuged at 12,000 *g* for 10 min at 4°C, and supernatants were collected. To estimate the GSH levels, the lyzed samples (90 μL/well) were transferred to 96-well black-bottom plates, mixed with a freshly prepared assay cocktail (10 μL), and incubated for 2 h. Thereafter, plates were read on an excitation wavelength at 380 nm and an emission wavelength at 460 nm using a Multiwell Microplate Reader (Synergy HT; Bio-Tek). The standard curve was plotted using the GSH standard supplied in the kit and used to calculate the experimental values.

Terminal deoxynucleotide transferase dUTP nick-end labeling assay. Apoptosis was detected by terminal deoxynucleotide transferase dUTP nick-end labeling (TUNEL) assays using the APO-BrdU TUNEL Assay Kit with Alexa-Fluor-488 anti-BrdU (Molecular Probes, Invitrogen Detection Technologies; Catalog No. A23210) by a flow cytometer (BD-LSRII) and analyzed by Cell Quest 3.3 software. Debris was excluded by forward and sideway light scattering. Positive and negative controls were provided along with the kit. Cells exposed to camptothecin (3 μg/mL) for 6 h were also used as positive controls.

Detection of mitochondrial membrane potential. Mitochondrial membrane potential, an early marker of apoptosis induction, was assessed using a Mitolight™ Apoptosis Detection Kit (APT142; Chemicon). Cells in culture (4×10^4 cells/well in a PLL-coated black-bottom 96-well plate) were exposed to MCP (10^{-5} M for 6 h). The medium was then aspirated, and cells were washed with DPB. Cells were then reincubated with 100 μL of prediluted Mitolight™ dye solution for 15 min (37°C, 5% CO_2–95% air) and allowed to equilibrate at room temperature for 10 min at dark. The fluorescence intensities were measured at an excitation wavelength 485 nm and an emission wavelength 530 nm to monitor monomer and wavelength 580 nm for aggregated molecules, respectively.

Transcriptional changes. Cells were exposed to MCP (10^{-5} M) for 3 h. Cells were then harvested and processed for real-time PCR. TaqMan Low Density Array of 48 genes was designed in 384-well plate formats and procured from Applied Biosystems (Table 1). MCP-induced alterations in the expression of mRNA of markers genes of stemness, proliferation, apoptosis, oxidative stress, and metabolism were analyzed using the ABI PRISM 7900HT Sequence Detection System (Applied Biosystems). The whole procedure was carried out by following the protocol as described by us earlier [22,23]. In brief, RNA was isolated from both MCP-exposed and unexposed cells using a GenElute mammalian total RNA Miniprep Kit (Catalog No. RTN-70; Sigma). The purity and yield of RNA were assessed by a Nanodrop ND-1000 Spectrophotometer V3.3 (Nanodrop Technologies, Inc.), and the quality was assessed by running RNA onto a 2% denaturing agarose gel. Total RNA (2 μg) was reverse-transcribed into cDNA using a SuperScript III first-strand cDNA synthesis Kit (Catalog No.18080-051; Invitrogen Life Science) and treated with RNase-free DNase I to remove any potential DNA contamination. cDNA was first preamplified using the primer pool provided by Applied Biosystems with a customized TaqMan Low Density Array as per the manufacturer's protocol. Quantitative real-time PCR was performed by using the ABI PRISM®7900HT Sequence Detection System (Applied Biosystems). Real-time reactions were carried out in triplicate. GAPDH was used as internal control to normalize the data. MCP-induced alterations in mRNA expressions of different genes are expressed in relative quantity compared with unexposed control groups.

Translational studies. Cells were exposed to MCP (10^{-5} M) for 6 h. The altered expression of marker proteins of apoptosis and cell death pathways was studied in both experimental and control groups. Proteins harvested from experimental and control groups were processed for western blot analysis following the protocol described earlier by us [22,23]. In brief, MCP-exposed and unexposed cells were pelleted and lyzed using the CelLytic™ Cell Lysis Reagent (Catalog No. C2978; Sigma) in the presence of 1× protein inhibitor cocktail (Catalog No. P8340; Sigma) and 1 mM sodium orthovanadate. After protein estimation by BCA Protein Assay (Catalog No. G1002; Lamda Biotech, Inc.), equal amounts (50 μg/well) of proteins were loaded in a 10% Tricine–SDS gel and blotted on a polyvinylidene fluoride membrane using a wet transfer system. After blocking for 2 h at 37°C, the membranes were incubated overnight at 4°C with specific antiprotein primary antibodies of PI3K (1:1,000), pGSK3β (Ser9), GSK3α/β, β-catenin, pAkt (Thr308) and pAkt (Ser473) (1:500), p-JNK (1:1,000); p53 and P21 (1:500), Bax (1:500), Bcl2 (1:1,000), and activated caspase-9 and 3 (1:500 and 1:200; Chemicon, Inc.; BD Biosciences; Santa Cruz) in a blocking buffer (pH 7.5). The membranes were then incubated for 2h at room temperature with a secondary antiprimary immunoglobulin-G conjugated with horseradish peroxidase (Calbiochem). The blots were developed using luminol (Cat. No. 34080; Thermo Scientific), and densitometry for protein-specific bands was done in a Gel Documentation System (Alpha Innotech) with the help of AlphaEaseTM FC StandAlone V. 4.0.0 software. Actin-β was used as the internal control to normalize the data. MCP-induced alterations in the expression of marker proteins are expressed in relative quantity compared with the unexposed control groups.

Activity of caspase-9 and 3. MCP-induced alterations in the activity of caspase-9 and caspase-3 were estimated using kits (Calbiochem; Catalog No. QIA72 and Biovision; Catalog No. K196, respectively). The exposure groups and conditions were identical to that of ROS and GSH. After respective exposures, cells were pelleted, resuspended in a prechilled extraction buffer (50 μL), and incubated for 10 min on ice. Then, the samples were centrifuged for 5 min at 500 *g*, and the clear supernatant (50 μL per well) was transferred to black-bottom 96-well culture plates for caspase-9, and

Table 1. Genes and Their Relevant Information Customized in TaqMan Low-Density Array Plate

S. No.	Assay Id	Gene symbol	Accession No.	Amplicon length
Stem cells				
1	Hs00156373_m1	*CD34*	2 RefSeqs	63
2	Hs00277045_m1	*CD38*	NM_001775.2	97
3	Hs00179843_m1	*SHH*	NM_000193.2	70
4	Hs03005111_g1	*POU5F1*	NM_002701.4	64
5	Hs00358836_m1	*KLF4*	NM_004235.3	110
6	Hs00153408_m1	*MYC*	NM_002467.3	107
Signaling				
7	Hs00180529_m1	*WNT1*	NM_005430.3	77
8	Hs02621230_s1	*PTEN*	NM_000314.4	135
9	Hs00234522_m1	*FRAP1*	NM_004958.3	71
10	Hs00765730_m1	*NFKB*	NM_003998.2	66
11	Hs00167223_m1	*NOS1*	NM_000620.2	61
12	Hs01047580_m1	*STAT3*	3 RefSeqs	87
13	Hs01028017_m1	*STAT4*	NM_003151.2	70
14	Hs01093077_m1	*COX10*	NM_001303.3	91
MAP kinases				
15	Hs00178726_m1	*ASK1*	NM_005923.3	138
16	Hs01052196_m1	*MAPK1*	NM_002745.4	66
17	Hs01548508_m1	*Mapk8*	4 RefSeqs	83
18	Hs00177102_m1	*MAPK9*	5 RefSeqs	102
19	Hs00373461_m1	*MAPK10*	10 REFSEQS	77
20	Hs00177101_m1	*MAPK11*	NM_002751.5	92
21	Hs99999141_s1	*JUN*	NM_002228.3	64
22	Hs00231713_m1	*CREB1*	2 RefSeqs	75
23	Hs00152928_m1	*EGR1*	NM_001964.2	72
24	Hs01119267_g1	*FOS*	NM_005252.2	67
Oxidative stress and metabolism				
25	Hs00169233_m1	*AHR*	NM_001621.3	105
26	Hs00153120_m1	*CYP1A1*	NM_000499.2	91
27	Hs03044636_m1	*CYP2B6*	NM_000767.4	125
28	Hs00164383_m1	*CYP1B1*	NM_000104.2	118
29	Hs00559367_m1	*CYP2E1*	NM_000773.3	71
30	Hs01070905_m1	*CYP3A5*	NM_000777.2	101
31	Hs00173566_m1	*GPX3*	NM_002084.3	90
32	Hs00156308_m1	*CAT*	NM_001752.2	68
33	Hs00167317_m1	*gsr*	NM_000637.2	63
34	Hs00533490_m1	*SOD1*	NM_000454.4	60
35	Hs00168310_m1	*GSTP1*	NM_000852.3	54
36	Hs00168315_m1	*GSTT2*	NM_000854.3	6
Apoptosis				
37	Hs00533490_m1	*SOD1*	NM_000454.4	60
38	Hs00162090_m1	*SOD3*	NM_003102.2	99
39	Hs00159041_m1	*MAP2*	NM_002374.3	59
40	Hs00241436_m1	*DRD2*	2 RefSeqs	64
41	Hs00609526_m1	*DRD4*	NM_000797.2	99
42	Hs00173566_m1	*GPX3*	NM_002084.3	90
43	Hs00168315_m1	*GSTT2*	NM_000854.3	6
44	Hs00156308_m1	*CAT*	NM_001752.2	68
45	Hs00826661_m1	*GSTO2*	NM_183239.1	139
46	Hs00168310_m1	*GSTP1*	NM_000852.3	54
Internal control				
47	Hs01922876_u1	*GAPDH*	NM_002046.3	139
48	Hs99999901_s1	*18S*	X03205.1	187

transparent-bottom plates for caspase-3 activity. Assay buffer (50 μL) and substrate conjugate (10 μL) for caspase-9 and (5 μL) for caspase-3 were added and mixed well. Upon the completion incubation of 2 h at 37°C in dark, contents were mixed thoroughly and read for fluorescence quantification on excitation at 400 nm and emission at 505 nm for caspase-9, whereas caspase-3 activity was measured by taking absorbance at 400 nm. The values of experimental groups were compared with the unexposed control group, and data expressed in fold change in activity.

Statistical analysis. Results were expressed as mean ± standard error of mean (SEM) for the values obtained from at

least 3 independent experiments. The level of significance for comparison between samples was ascertained using the Student's *t*-test distribution. For recovery experiments, 1-way ANOVA, followed by post hoc Tukey's b test, was used. The data in the graphs are expressed as the mean ± SEM. Graphpad Prism 3.0 software (Graphpad Software) was used for all the statistical analyses. The values $P < 0.05$ were considered to be significant.

Results

In silico molecular docking analysis of MCP

The aim of the molecular docking study was to elucidate whether the test compound MCP modulates the cell survival protein kinase B (Pkb/Akt), and to study their possible mechanisms of action. The results of the molecular docking suggest that the studied compound binds strongly with the kinase and C-terminal regulatory domains of Akt at a region that also serves as an ATP-binding pocket. In the work presented here, we explored the orientation and binding affinity [in terms of the total score in $-\log_{10}$ (Kd) units to represent binding affinities] of camptothecin and MCP toward the anticancer target Akt kinase (PDB code: 3CQU). The docking reliability was validated using the known crystalline X-ray structure of Akt kinase complexed with the pyrrolopyrimidine inhibitor. The co-crystallized pyrrolopyrimidine inhibitor was redocked into the binding site, and the docked conformation with the highest total score of 7.7894 was considered as the most probable binding conformation. The low root mean-square deviation of 0.3769 Å between the docked and the crystal conformation indicates the high reliability of Surflex-dock software in reproducing the experimentally observed binding mode for this inhibitor. As shown in Fig. 1, redocked molecules were almost in the same position with co-crystallized at the active site of the pyrrolopyrimidine inhibitor (Fig. 1A).

On the other hand, docking results for camptothecin against the anticancer/survival target protein Akt kinase showed a high binding affinity docking score indicated by a total score of 5.7543 and forms a H-bond of length 2.1 Å to the hydrophobic aliphatic residue that is, Alanine 230. In the docking pose of the camptothecin–Akt complex, the chemical nature of binding site residues within a radius of 4 Å was basic (polar, hydrophobic, positive charged), for example, Arg-4 (Arginine) and Lys-276 (Lysine); aromatic (hydrophobic), for example, Phe-161, Phe-438 (Phenylalanine), and Tyr-229 (Tyrosine); acidic (polar, negative charged), for example, Glu-228 (Glutamic acid) and Asp-292 (Aspartic acid); polar amide type, for example, Asn-279 (Asparagine); hydrophobic, for example, Ala-177, Ala-230 (Alanine), Gly-157 (Glycine), Leu-156 (Leucine), Met-227, and Met-281 (Methionine); and nucleophilic (polar, hydrophobic), for example, Thr-211 and Thr-291 (Threonine); as a result, the bound compound showed a strong hydrophobic interaction with Akt kinase, thus leading to more stability and activity in this compound (Fig. 1B).

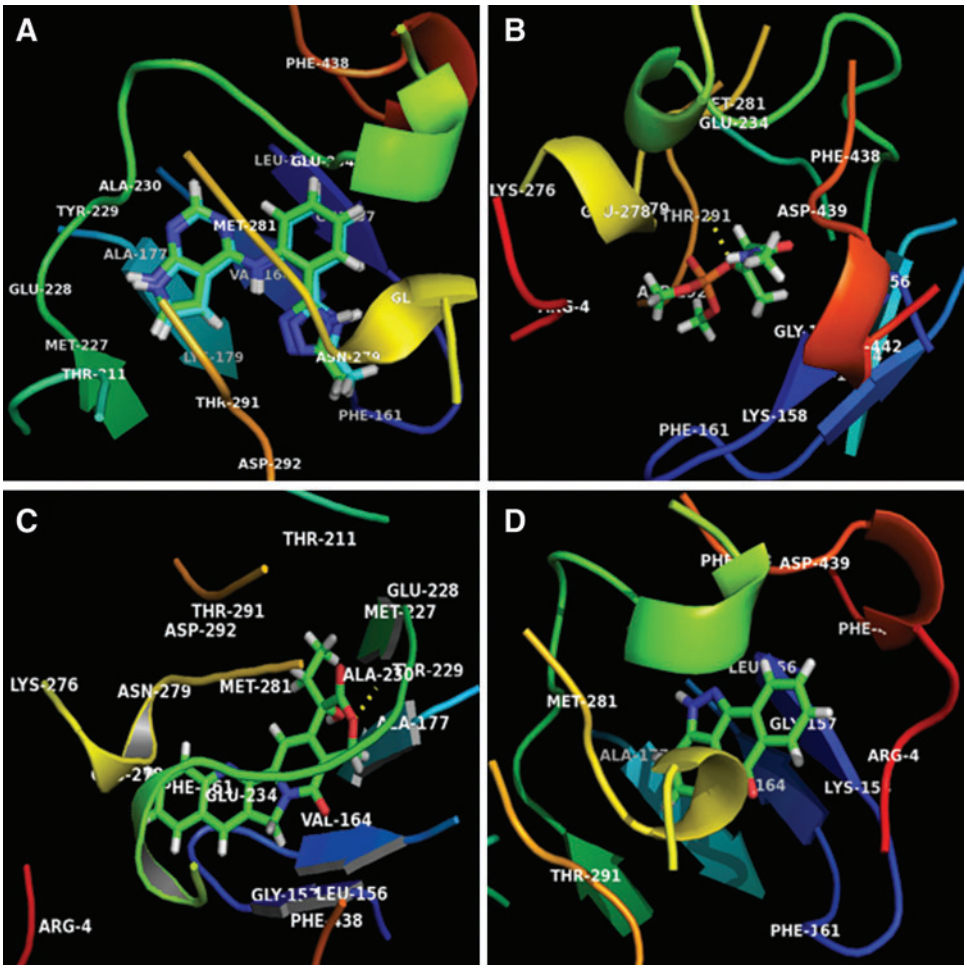

FIG. 1. In silico molecular docking studies elucidating the possible mechanisms of monocrotophos (MCP)-induced modulation of cell survival protein kinase B (Pkb/Akt). The docking studies were carried out using SYBYL-X 1.3, Tripos International. **(A)** The co-crystallized pyrrolopyrimidine inhibitor was redocked into the binding site of Akt kinase (PDB: 3CQU) with 0.3769 Å of root mean-square deviation between docked and crystallized conformation and a total docking score of 7.7894. **(B)** MCP docked on to Akt kinase (PDB: 3CQU) with high binding affinity, as indicated by a total docking score of 5.2748 compared to camptothecin. **(C)** Camptothecin docked on to Akt kinase (PDB: 3CQU) with high binding affinity, as indicated by a total docking score of 5.7543. **(D)** SP600125 docked on to Akt kinase (PDB: 3CQU) with a low binding affinity, as indicated by a total docking score of 4.6662. Color images available online at www.liebertpub.com/scd

The binding affinity obtained in the docking study allowed a comparison between the activities of the MCP to be compared to that of the standard anticancer drug camptothecin. MCP showed a high binding affinity against the Akt kinase target protein. During the comparison of the nature of interaction between the binding pocket amino acid residues of target protein and the compound, it was found that the compound MCP showed molecular interaction with conserved hydrophobic amino acid residues, thus leading to more stability and potency (Table 2). The docking results for MCP showed that the compound docked on the anticancer target Akt kinase with a high binding affinity docking score indicated by its total score of 5.2748 and also showed the formation of a H-bond of length 2.3 Å to the hydrophobic nucleophilic (small, polar) residue Threonine, that is, Thr-291. The MCP-Akt-docked complex also showed a similar type of binding site residues within a radius of 4 Å of bound ligand such as basic (polar, hydrophobic, positive charged) residues, for example, Arg-4 (Arginine), Lys-158, and Lys-179 (Lysine); aromatic (hydrophobic) residues, for example, Phe-161, Phe-438, and Phe-442 (Phenylalanine); acidic (polar, negative charged) residues, for example, Glu-234, Glu-278 (Glutamic acid), Asp-292, and Asp-439 (Aspartic acid); polar amide type residue, for example, Asn-279 (Asparagine); hydrophobic residue, for example, Met-281 (Methionine); and nucleophilic (polar, hydrophobic) residue, for example, Thr-291 (Threonine), compared to camptothecin; therefore, the docked molecule also showed a strong hydrophobic interaction with Akt kinase, thus leading to more stability (Fig. 1C).

The docking results for the negative control molecule SP600125 (JNK inhibitor) with the anticancer/survival target protein Akt kinase showed a low binding affinity docking score, indicated by a low total score of 4.6662 without any H-bond (hydrogen bond) formation (Fig. 1D), in comparison to the docking score of anticancer known inhibitors such as pyrrolopyrimidine and camptothecin, which showed a total score of 7.7894 and 5.7543, respectively (Table 2). Thus, the docking procedure of Surflex-dock software (Sybyl-X 1.3) in reproducing the experimental binding affinity seems reliable, and therefore predicted as true positive.

In vitro validation studies

Isolation, purification, and characterization of umbilical cord blood stem cells. In the first instance, isolated stem cells were 60%–85% purified and having more than 85%–90% viability. Cells were showing the expression of surface markers CD34 (77.35% ± 13.04% cells) and Thy1 (69.77% ± 12.32% cells) (Fig. 2A, B). In a myelocult culture medium supplemented with the cocktail of specific growth factors and cytokines, the purity of stem cells showing these markers was increased with further passages. The purified population of stem cells could be maintained for more than 3 months up to 10–12 passages. During cultivation, a progressive cell proliferation with cluster formation was observed (Fig. 2C). Upon breaking, individual small rounded cells increased in size and formed large colonies within the time of a week. Some single cells and colonies were found to be adhered on to the substratum of the culture flask. Numerous cells within adhered clusters started to send out tiny processes, and later on, clearly distinct cell types appeared. They tightly adhered

Table 2. Comparison of Docking Score and Binding-Site Residues of Studied Compounds Against the Target Akt1 Kinase

S. No	*Compound*	*Total score*	*Biding pocket residue in (4 Å)*	*Length of hydrogen bond (Å)*	*Amino acid residue involved in docking interaction*	*No. of hydrogen bond (H)*
1.	Compound-SP600125 (negative control)	4.6662	ARG-4, LEU-156, GLY-157, LYS 158, PHE 161, VAL-164, ALA-177, GLU-234, THR-291, PHE-438, ASP-439, PHE-442	—	—	—
2.	Camptothecin (positive control)	5.7543	ARG-4, LEU-156, GLY-157, PHE-161, ALA-177, THR-211, MET-227, GLU-228, TYR-229, ALA-230, LYS-276, ASN-279, MET-281, THR-291, ASP-292, PHE-438	2.1	ALA-230	1
3.	Monocrotophos (test compound)	5.2748	ARG-4, LYS-158, PHE-161, LYS-179, GLU-234, GLU-278, ASN-279, MET-281, THR-291, ASP-292, PHE-438, ASP-439, PHE-442	2.3	THR-291	1

Surflex-Dock scores (total scores) were expressed in $-\log_{10}$ (Kd) units to represent binding affinities.

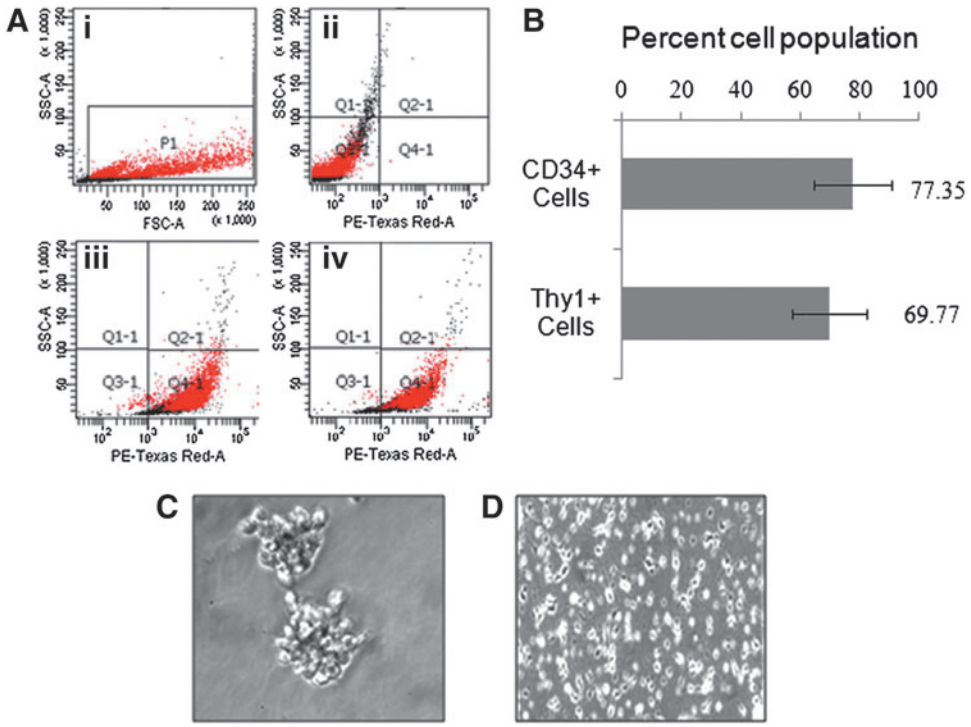

FIG. 2. Purification and characterization of human umbilical cord blood stem cells. **(A)** Selected cell population **(i)**; unstained umbilical cord blood stem cells **(ii)**; cells stained with PE-Texas Red-conjugated $CD34^+$ **(iii)**; and $Thy1^+/CD90^+$ antibodies **(iv). (B)** The percent cell population expressing $CD34^+$ and $Thy1^+/CD90^+$ surface markers of pluripotency. **(C)** Purified clonal population growing in bunches/microspheres. **(D)** Proliferative single-cell population derived from the dissociated microspheres. Color images available online at www.liebertpub.com/scd

to the surface of the culture flask and frequently had numerous small cells on their surface or in close vicinity to the cell (Fig. 2D). The cells grown under deprivation of growth factors and cytokines were decreased in number and could survive.

Cytotoxicity studies

Prior using in the experiments, biologically safe doses of MCP were identified using tetrazolium bromide salt (MTT) and LDH-release assays. In MTT assay, no significant cytotoxic response was recorded until 24-h exposure, except for MCP 10^{-3} M concentration. Thereafter, a dose-dependent decrease in the percent cell viability was observed till the end of exposure, that is, 96 h. In general, MCP (10^{-3} and 10^{-4} M) exposure for 48 h and onward were found cytotoxic, whereas, rest of the concentrations of MCP used in the study were safe until 48 h (Fig. 3A). Data of LDH-release assay were also showing a similar trend (Fig. 3A, B). Based on these results, further experimentations were carried out using a safe dose of MCP (10^{-5} M) for 3 h (RNA expression studies) and 6 h (protein expression and apoptosis studies).

Oxidative stress

ROS generation. MCP exposure for 6 h shows statistically significant ($P < 0.001$) generation of ROS in cells, that is, 227.6% ± 6.3% of control. Similarly, the positive control camptothecin has also induced significant ROS generation 209.3% ± 4.6% of control. Cells receiving the co-exposure of MCP and NAC (known antioxidant) show the significant ($P < 0.001$) restoration (126.3 ± 5.21 of control) in ROS levels, when compared with MCP-alone exposure (Fig. 4A).

Intracellular GSH levels. A significant ($P < 0.05$) reduction (23.2 ± 0.6 mM) in the levels of intracellular GSH was observed in MCP- (10^{-5} M for 6 h) exposed cells when compared with the unexposed control cells (35.5 ± 1.2 mM). NAC was found to counteract the GSH-diminishing activity of MCP, as cells receiving the coexposure of MCP and NAC show the significant ($P < 0.05$) restoration (33.1 ± 0.8) in GSH levels. As anticipated,

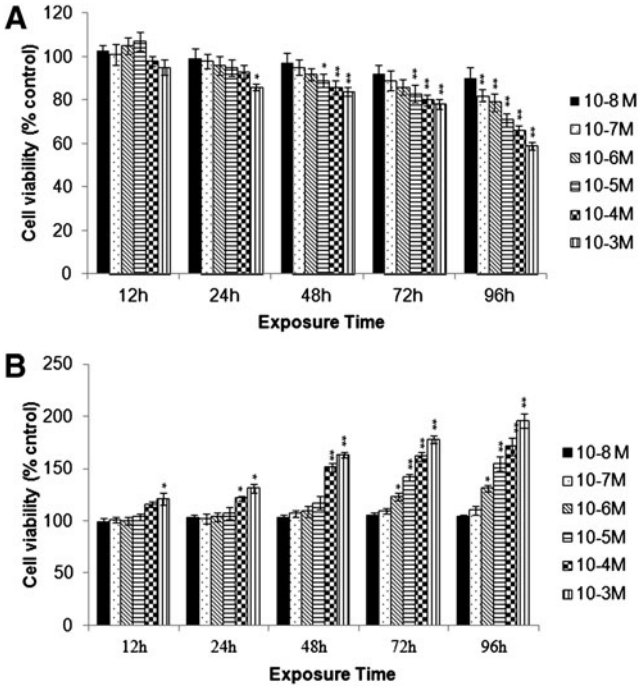

FIG. 3. Identification of noncytotoxic doses of MCP, an organophosphate pesticide. Cells were exposed to MCP (10^{-3} to 10^{-8} M) for a period of 12–96 h. *$P < 0.05$; **$P < 0.001$. **(A)** Tetrazolium bromide salt 3-(4,5-dimethylthiazol-2-yl)-2,5-diphenyltetrazoliumbromide (MTT) assay. **(B)** Lactate dehydrogenase (LDH)-release assay.

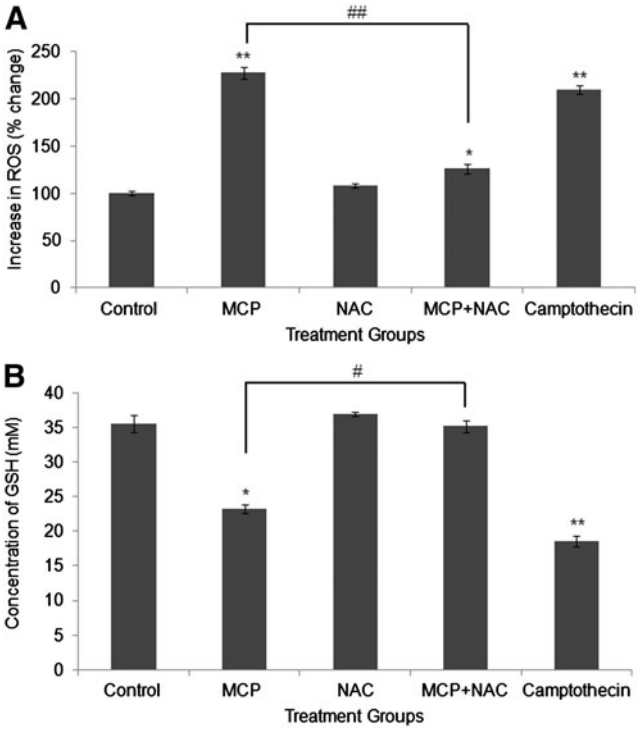

FIG. 4. MCP-induced oxidative stress analysis and ameliorative responses of N-acetylcysteine (NAC) in cultured human umbilical cord blood stem cells. **(A)** Estimation of MCP-induced reactive oxygen species (ROS) generation 2′, 7′ dichlorodihydrofluorescein-diacetate (DCFH-DA) method. Camptothecin (3 μg/mL) was used as positive control. $^{*}P < 0.05$; $^{**}P < 0.001$ (control vs. exposure groups); $^{\#\#}P < 0.001$ (MCP exposure vs. coexposure of MCP + NAC). **(B)** Estimation of intracellular glutathione (GSH) levels. $^{*}P < 0.05$; $^{**}P < 0.001$ (control vs. exposure groups); $^{\#}P < 0.05$; (MCP exposure vs. coexposure of MCP + NAC).

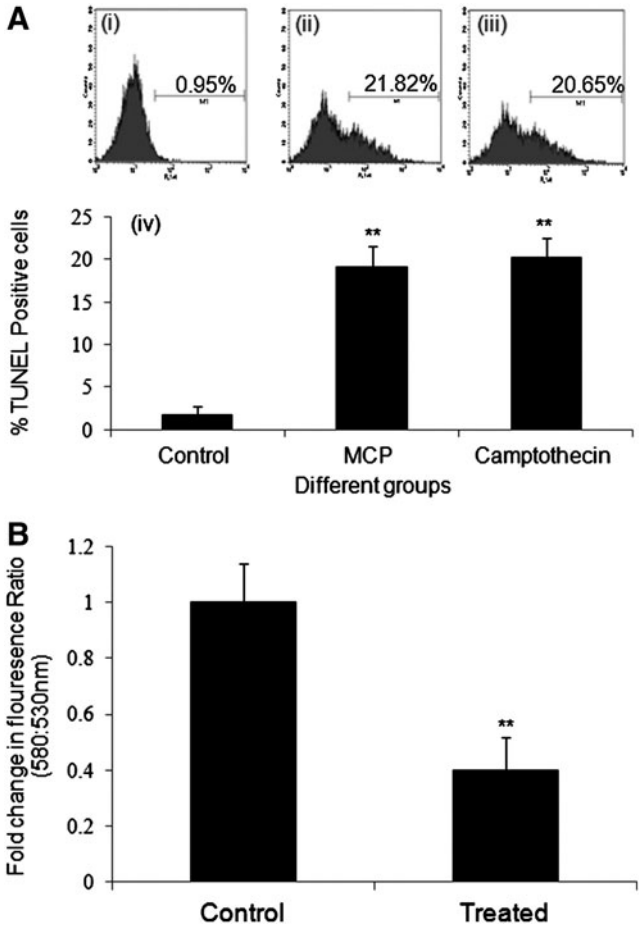

FIG. 5. Detection of apoptosis in cultured human umbilical cord blood stem cells exposed to MCP (10^{-5} M) for 6 h. **(A)** Apoptosis was detected by terminal deoxynucleotide transferase dUTP nick-end labeling (TUNEL) assays using APO-BrdU TUNEL Assay Kit with Alexa-Fluor-488 anti-BrdU (Molecular Probes, Invitrogen Detection Technologies; catalog no. A23210) by a flow cytometer (BD-LSRII) and analyzed by Cell Quest 3.3 software. **(i)** Unexposed control population of human umbilical cord blood stem cells. **(ii)** Human umbilical cord blood stem cells exposed to MCP (10^{-5} M) for 6 h. **(iii)** Human umbilical cord blood stem cells exposed to Camptothecin (3 μ\m) for 6 h as positive control. **(iv)** Graphical representation of mean ± SE values of triplicate experiments carried out for detection of apoptosis induction. **(B)** Graphical representation of early apoptosis induction in cultured human umbilical cord blood stem cells exposed to MCP (10^{-5} M) for 6 h by detecting the loss of mitochondrial membrane potential (MMP). MMP was detected using Mitolight™ Apoptosis Detection Kit (APT142; Chemicon). The fluorescence intensities were measured at excitation wavelength 485 nm and emission wavelength 530 nm to monitor monomer and wavelength 580 nm for aggregated molecules, respectively. $^{**}P < 0.001$.

a highly significant ($P < 0.001$) reduction (18.5 ± 0.8 mM) in the levels of GSH was recorded in cells exposed to the positive control camptothecin (Fig. 4B).

Induction of apoptosis

Our results from TUNEL assays indicate that MCP (10^{-5} M) exposure for 6 h induced significant apoptosis (19.14% ± 2.35%) in an exposed population of cells compared to 1.78% ± 0.93% control. Cells exposed to camptothecin (3 μg/mL) for 6 h have also shown the significant apoptosis (20.15% ± 2.34%) (Fig. 5A). A significant decrease (0.4-fold ± 0.12-fold of control) in the mitochondrial membrane potential was also observed using Mitolight™ dye in the cells exposed to identical conditions as exposed for the TUNEL assay (Fig. 5B).

Transcriptional studies

The results of MCP- (10^{-5} M for 3 h) induced alterations in the expression of markers of stemness, cell signaling, MAP kinases, apoptosis, oxidative stress, and metabolism are summarized in Fig. 6A–E. MCP exposure induces significant downregulation [CD34 (0.068E-06-fold of control) and SHH (8.44E-04-fold of control)] and upregulation [KLF4 (3.75 ± 0.43-fold of control) and POU5F1 (5.93 ± 1.3-fold of control)] of stemness genes studied (Fig. 6A). All the examined signaling genes studied were also found to be upregulated [mTOR (2.46 ± 0.21-fold), NFκB (1.81 ± 0.17-fold), NOS (6.05 ± 0.53-fold), STAT3 (1.87 ± 0.13-fold), and STAT4 (3.32 ± 0.14) of unexposed control], except in case of WNT1, where the expression was downregulated significantly

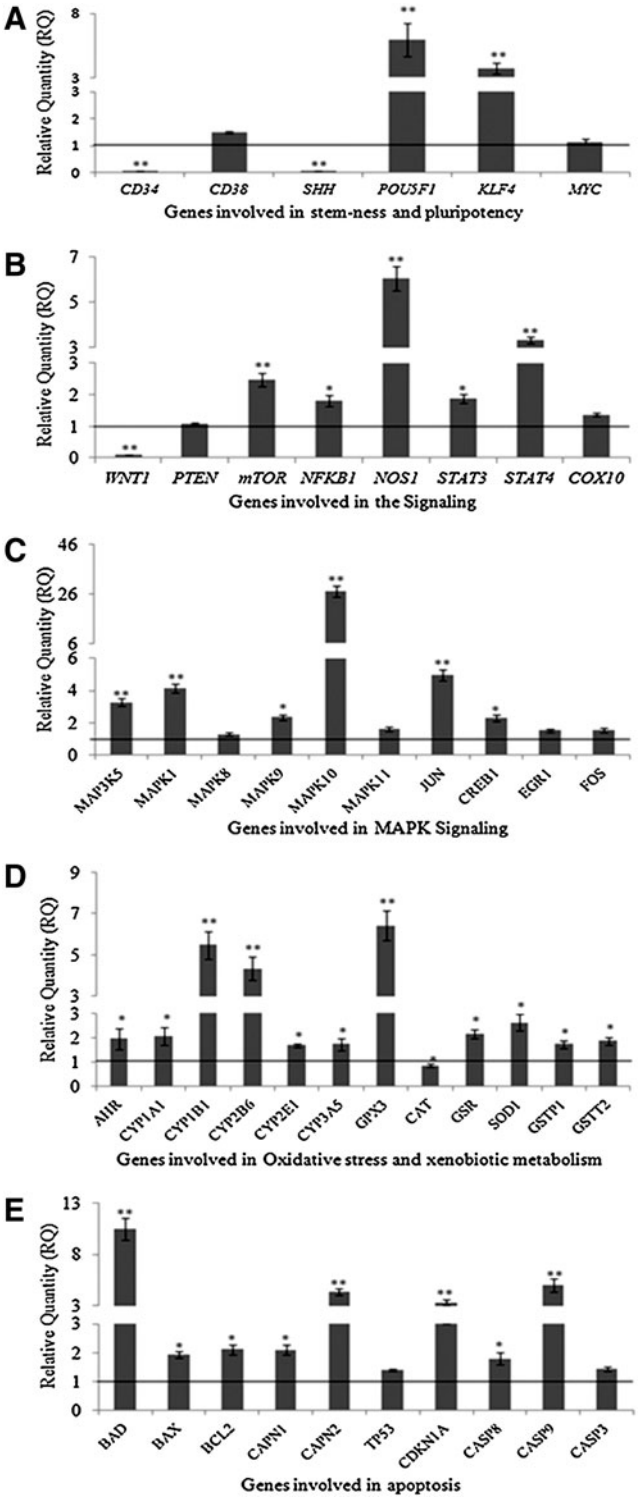

FIG. 6. Assessment of transcriptional changes in the selected marker genes of stemness, proliferation, signaling, apoptosis, oxidative stress, and metabolism in cultured human umbilical cord blood stem cells exposed to MCP (10^{-5} M) for 3 h. Real-time PCR was done using TaqMan Low Density Array designed in a 384-well plate format (Applied Biosystems). Analysis was done in ABI PRISM 7900HT Sequence Detection System (Applied Biosystems). *$P < 0.05$; **$P < 0.001$.

(8.17 ± 04-fold of control) (Fig. 6B). MCP exposure also induced upregulation of MAP kinases significantly, that is, MAPK10 (27.07 ± 2.1-fold), c-JUN (4.95 ± 0.32-fold), MAPK1 (4.14 ± 0.27-fold), MAK3K5 (3.27 ± 0.22-fold), MAPK9 (2.34 ± 0.16-fold), and CREB1 (2.294.95 ± 0.18-fold) of control (Fig. 6C). MCP-induced changes were also found to be associated with xenobiotic metabolizing cytochrome P450s and genes involved in oxidative stress as evidenced by significant ($P < 0.05$) alterations in the expression of these genes, that is, upregulation of CYP2B1 (5.46 ± 0.67-fold), CYP2B6 (4.33 ± 0.58-fold), CYP1A1 (2.05 ± 0.37-fold), GPX3 (6.40 ± 0.72-fold), GSR (2.16 ± 0.17), SOD1 (2.62 ± 0.34) and downregulation of CAT (0.84 ± 0.07-fold) (Fig. 6D). Similar to other genes, all the apoptosis marker genes were significantly upregulated ($P < 0.05$), that is, Bad (10.45 ± 1.10-fold), caspase-9 (4.99 ± 0.62-fold), CAPN1/2 (2.10 ± 0.16/4.03 ± 0.32), Bcl2 (2.10 ± 0.17-fold), Bax (1.93 ± 0.11-fold), and CDKN1A (3.27 ± 0.27-fold) of control, except caspase-3 (Fig. 6E).

Translational changes in marker proteins in differentiating cells exposed to MCP

The western blot analysis results of MCP- (10^{-5} M for 6 h) induced changes in the expression of markers involved in PI3K/Akt/GSK3β/β-catenin signaling and apoptosis in hUCBSCs are summarized in Fig. 7A–E. In general, MCP significantly downregulates the expression of pAkt (Thr308/Ser473)/pGSK3β (ser9)/β-catenin in hUCBSCs. The magnitude of alterations was also similar for camptothecin, a positive control used in the study. Although both MCP and camptothecin induce alterations in the expression of PI3k and nonphosphorylated GSK3α/β, the changes were statistically nonsignificant. However, a significant downregulation in the expression of survival protein β-catenin was observed in cells exposed to MCP/camptothecin. Stem cells responded significantly to MCP exposure in terms of apoptosis markers viz., pJNK1/2, c-JUN, P^{53}, Bax, and caspase 9/3. Pretreatment of SP600125, an inhibitor of JNK1/2, was found effective to control the altered expression of proapoptotic marker proteins viz., JNK1/2, c-JUN, p53, p21, BAX, and CASP 9/3, in hUCBSCs exposed to MCP.

Activity of caspase-9 and 3

The results of MCP-induced alterations in the activity of caspase-9 and 3 and ameliorative responses of NAC are summarized in Fig. 8A and B, respectively. MCP exposure (10^{-5} M for 6 h) significantly ($P < 0.001$) induces the activity of caspase-9 (3.43 ± 0.4-fold of control). NAC was found effective to ameliorate the activity responses significantly ($P < 0.05$), as co-exposure of MCP + NAC brought down the caspase-9 activity near to the unexposed control, that is, 1.80 ± 0.05-fold of control (Fig. 8A). The trend for the activity of caspase-3 was similar to that of caspase-9; however, the magnitude of induction was comparatively lower, that is, 2.63 ± 0.11-fold of control. The ameliorative response of NAC to the activity of caspase-3 was also more or less similar (1.53 ± 0.08-fold of control) to that of caspase-9 (Fig. 8B).

Discussion

In our earlier studies, we have shown that MCP induces mitochondrial-mediated apoptosis and association of

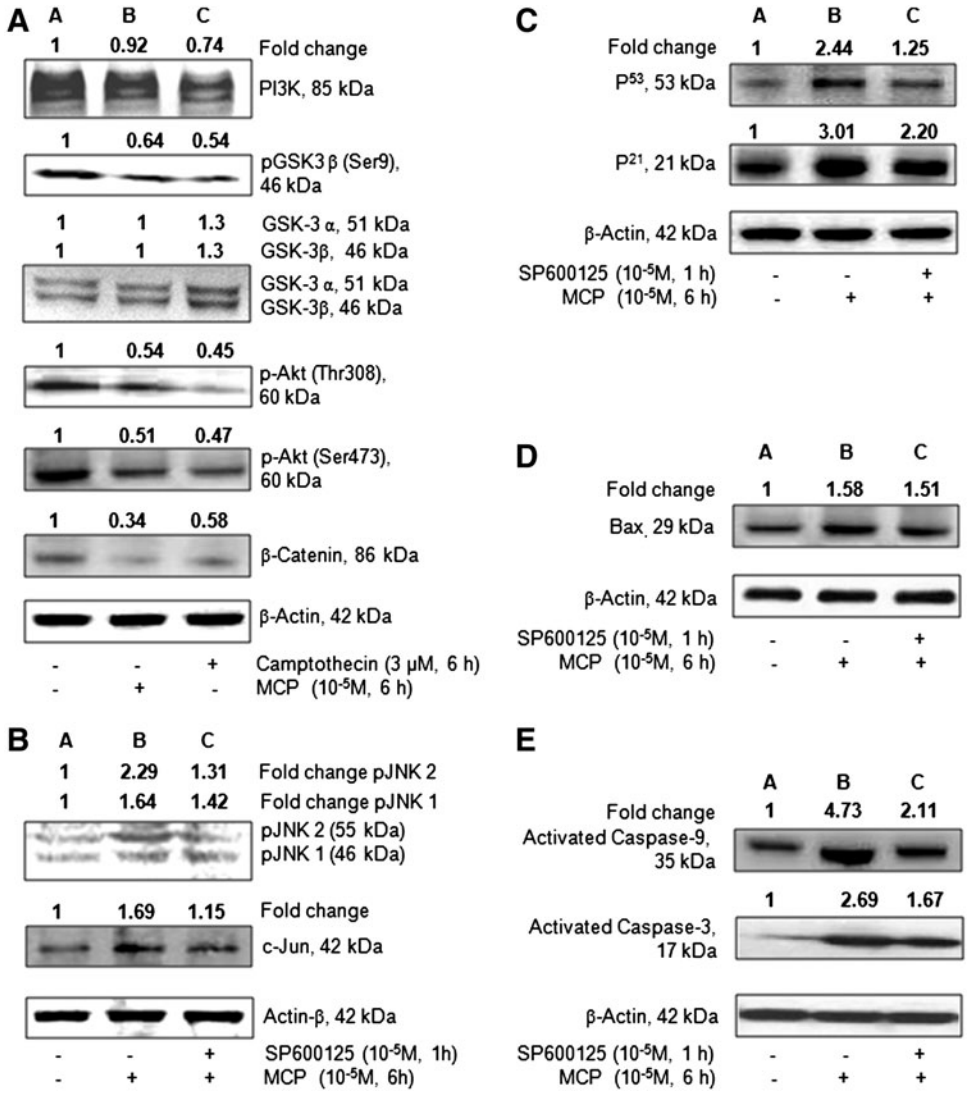

FIG. 7. Western blot analysis to study the translational changes in the selected marker markers involved in phosphoinositide 3-kinase (PI3K)/Akt/GSK3β/β-catenin signaling and apoptosis in cultured human umbilical cord blood stem cells exposed to MCP (10^{-5} M) for 6 h. **(A)** Analysis of MCP-induced alterations in protein expression of PI3K, pGSK3β (Ser9), GSK3α/β, pAkt (Thr 308), pAkt (Ser473), and β- catenin. The data were compared with positive (camptothecin) and negative (unexposed) controls. *Lane A:* unexposed control cells; *Lane B:* MCP-exposed cells; *Lane C:* cells exposed to camptothecin. **(B)** Analysis of MCP-induced alterations in protein expression of MAPKs viz., pJNK1, pJNK2, and c-Jun. *Lane A:* unexposed control cells; *Lane B:* MCP (10^{-5} M) exposure for 6 h; *Lane C:* cells pretreated with a specific inhibitor of JNK1/2 [SP600125 (10 μM)] for 1 h, washed, and then re-exposed to MCP (10^{-5} M) for 6 h. **(C)** Analysis of MCP-induced alterations in protein expression of apoptotic regulators viz., p53 and p21. *Lane A:* unexposed control cells; *Lane B:* MCP (10^{-5} M) exposure for 6 h; *Lane C:* cells pretreated with a specific inhibitor of JNK1/2 [SP600125 (10 μM)] for 1 h, washed, and then re-exposed to MCP (10^{-5} M) for 6 h. **(D)** Analysis of MCP-induced alterations in protein expression of proapoptotic marker Bax. *Lane A:* unexposed control cells; *Lane B:* MCP (10^{-5} M) exposure for 6 h; *Lane C:* cells pretreated with a specific inhibitor of JNK1/2 [SP600125 (10 μM)] for 1 h, washed, and then re-exposed to MCP (10^{-5} M) for 6 h. **(E)** Analysis of MCP-induced alterations in protein expression of activated caspases-9 and 3. *Lane A:* unexposed control cells; *Lane B:* MCP (10^{-5} M) exposure for 6 h; *Lane C*: cells pretreated with a specific inhibitor of JNK1/2 [SP600125 (10 μM)] for 1 h, washed, and then re-exposed to MCP (10^{-5} M) for 6 h.

xenobiotic-metabolizing P450s in rat pheochromocytoma (PC12) cells. We have also demonstrated the altered expression and possible association of selected xenobiotic-metabolizing cytochrome P450s with MCP-induced damages in the same cells [22,23]. In the present investigations, we used the primary cultures of human hematopoietic stem cells derived from cord blood to investigate the responsiveness of these cells against MCP exposure. Thus, with the background knowledge generated on apoptotic responses of MCP in PC12 cells, the present study is focused to explore the role of protein kinase-B in the regulation of apoptosis in human hematopoietic stem cells. Hematopoietic stem cells used in the study were isolated from human umbilical cord blood, as it is a noninvasive, rich source of $CD34^{+}CD38^{-}$

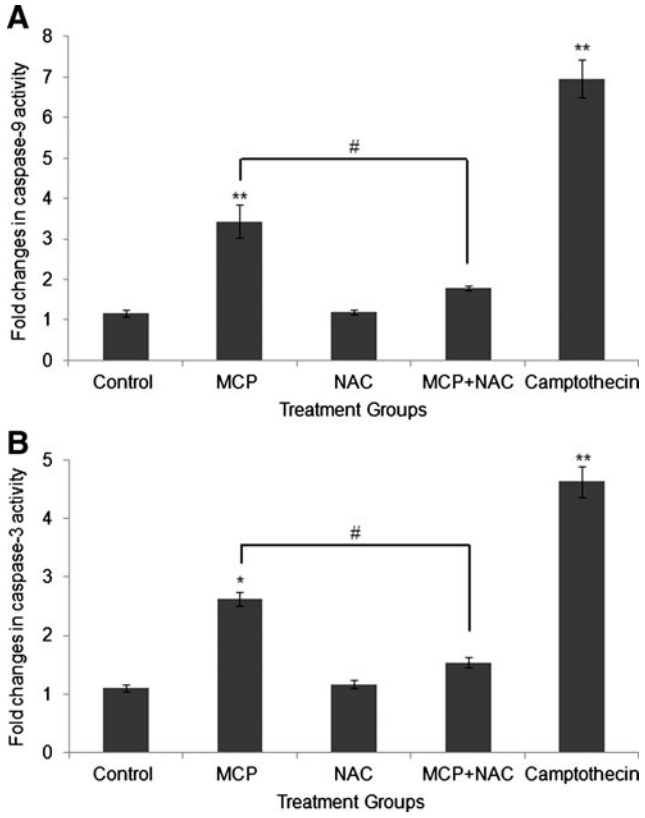

FIG. 8. MCP-induced alterations and ameliorative responses of NAC on the activity of caspase-9 **(A)** and caspase-3 **(B)** in cultured human umbilical cord blood stem cells. Camptothecin (3 μg/mL) was used as positive control. Values are expressed in fold change of control. $^{*}P < 0.05$; $^{**}P < 0.001$ (control vs. exposure groups); $^{\#}P < 0.05$; (MCP exposure vs. co exposure of MCP + NAC).

stem cells [28–30]. In general, a range from 0.6% to 1.35% ($N = 52$) of $CD34^{+}$ stem cells could be isolated with the viability of 90%–95%. A number of reasons might be responsible for the loss of 5%–10% viability during sample processing such as blood storage time, magnetic effects during processing, addition of an antiblood coagulant, etc. Also, the other factors like gestational age, mode of delivery, and positioning of neonate after delivery have also found to be associated with variation in the number of hematopoietic stem cells [31,32]. Using permutation of combination of various cytokines/growth factors, viz., TPO, FLT-3 ligand, SCF, and FGF-basic, cells could be cultured in a proliferative stage up to 4-month time. This suggests the extensive self-renewal and undifferentiated proliferation capacity of cultured hematopoietic stem cells for such a prolonged period of time.

In the present investigations, human hematopoietic stem cells responded against MCP exposure similar to that of PC12 cells [22,23], Caco-2 cells [33], and peripheral blood lymphocytes [34,35]. Since, the MCP-induced alterations in the expression of markers of oxidative stress, apoptosis, and xenobiotic-metabolizing cytochrome P450s in hUCBSCs were comparable to our earlier findings with PC12 cells [22,23]. Based on the findings, we hypothesized the involvement of Akt, also known as Pkb, in the regulation of signaling of the whole cascade of MCP-induced apoptosis and cell injury in hUCBSCs. The hypothesis was based on the established role of Akt in the suppression of apoptosis by inhibiting the proteins involved in cell death, including ASK1/caspase-9/Bad/P^{53} and P^{21} and promoting the cell survival pathway, including IGF-1R/PI3K/PTEN/mTOR [4]. However, such findings related to Akt are largely considered as its anticancerous phenomenon property and looked into cancerous-related studies only [5,12,14–16]. Perhaps, the role of Akt in the regulation of xenobiotics-induced apoptosis and injury in hUCBSCs is being reported for the first time. To prove the hypothesis, molecular docking studies were carried out to elucidate whether the test compound MCP modulates the anticancer target Pkb/Akt, and to study the possible mechanisms of action. The docking results were further validated using the expression (mRNA and protein) studies for markers of apoptosis, cell injury, selected CYPs, and Akt signaling pathways.

The binding affinity obtained in the docking study allowed the activity of the MCP compared to that of the standard anticancer drug camptothecin. MCP showed high binding affinity against the Akt kinase target protein. When we compared how the binding pocket amino acid residues of target protein interacted with the compound, we found that the compound MCP has molecular interaction with conserved hydrophobic amino acid residues, thus leading to more stability and potency. The docking results for MCP showed that the compound docked onto the anticancer target Akt kinase with a high binding affinity docking score and also formed H-bond of length 2.3 Å to the hydrophobic nucleophilic (small, polar) residue Threonine, that is, Thr-291, similar to that of camptothecin. To better understand the binding nature of MCP to Akt, the MCP-Akt-docked structure was compared with the presolved X-ray co-crystal structure of the Akt–imidazopiperidine analog (8b) and anilinotriazole analog 5d [5]. Most notably, MCP interacts with Glu-234 and Asp-292 and forms a hydrogen bond between N-H and Thr-291 of Akt in the vicinity of where the ribose of ATP would normally occupy. Similar types of findings have been observed in the imidazopiperidine analog 8b, in which the protonated imidazole nitrogens involve in 2 hydrogen bonds between Glu-234 and Asp-292 [5]. In addition, Phe-161 was also found to interact with MCP as in the case of the imidazopiperidine analog (8b), which pi-stacked with the anilinotriazole analog 5d, resulting in a significant conformational change in this portion of the protein [5]. Gurbani et al. [36] has also reported a similar type of mechanism of inhibition of the ATPase domain of Human Topoisomerase IIα (TopoIIα) by different quinone analogs. They showed the interaction with Ser-148, Ser-149, Asn-150, and Asn-91 residues of the ATPase domain of Hu-TopoIIα with quinone analogs viz., 1, 4-benzoquinone, 1, 2-naphthoquinone, 1, 4-naphthoquinone, and 9, 10-phenanthroquinone [36]. The combined results of molecular docking and western blot analysis suggest that MCP significantly inhibits the activity of Akt kinase by hampering the phosphorylation at Thr308/Ser 473, which may be due to interactions at the ATP vicinity and works as a selective, ATP-competitive inhibitor of Akt [5,37].

Our wet laboratory data confirm the in silico finding that MCP significantly reduces the phosphorylation of Akt at both the domains at position Thr308 and Ser473 position. Phosphorylated/activated Akt inactivates the GSK3β by phosphorylating it at Ser9 [4]. In our studies, the reduced

levels of phosphorylated GSK3-β (Ser9) and unaffected levels of nonphosphorylated GSK3β suggest the degradation of beta-catenin through an ubiquitin-dependent proteasome pathway, which leads to apoptotic cell death [38]. The activation of GSK3β is also known to inhibit the Wnt/frizzled/disheveled (DSH) pathway to promote cell survival and growth [38]. Thus, the reduced levels of pAkt, Wnt, and β-catenin observed in present study may also indicate to cause the impaired Wnt/Akt/β catenin signaling and subsequent induction of apoptosis in hUCBSCs exposed to MCP. Unaltered levels of PTEN and PI3K confirm the involvement of other routes of pAkt inhibition in MCP-induced cell death signals in hUCBSCs. Phosphorylation of Akt (Ser473) at the AGC-kinase C-terminal regulatory domain via mTOR plays an important role in triggering the signals of cell survival/growth [4]. Our in silico data show that MCP binds with the Akt AGC-kinase C-terminal regulatory domain, so causes the hindrance in phosphorylation of Akt (Ser473). This might be the reason that even after significant upregulation in the levels of mTOR/FRAP1, there was no sufficient phosphorylation in Akt (Ser473) in MCP-exposed hUCBSCs.

The protective role of pAkt is reported primarily by NFκB survival signaling, thereby inhibiting ASK1, which eventually blocks the phosphorylation of downstream JNK1/2 [4]. Such elevated levels of pJNK1/2 have been reported to induce apoptosis via the activation of downstream molecules viz., P^{53}, P^{21}, Bax, and caspases, in a variety of cells [22,23,39]. In agreement to the earlier findings, present investigations also confirm the upregulation of NFκB, ASK1, and p-JNK1/2 expression in MCP-exposed hUCBSCs. Our study related to a JNK inhibitor (SP600125) also indicates the involvement of ASK1 and p-JNK1/2 pathways in causation of apoptosis mediated through P^{53}, P^{21}, Bax, and caspases 9/3. Our findings are indicating that MCP-induced apoptosis also involve the pathways of oxidative stress and xenobiotic metabolism. Earlier, we have reported the association of oxidative stress and xenobiotic-metabolizing cytochrome P450s in the mitochondrial-mediated apoptosis induced by MCP in PC12 cells [22,23].

Bad, a soluble proapoptotic protein, interacts with the antiapoptotic proteins Bcl-2/Bcl-xL into the mitochondrial membrane, and prevents the antiapoptotic activity of these proteins via preventing the interaction of proapoptotic Bax with these proteins [4,39]. As a result, Bax creates homo-oligomeric channels in the mitochondrial membrane and leads to the release of cytochrome-*c* from the mitochondria to the cytoplasm. Cytochrome-*c* interacts with the adapter protein Apaf-1, which leads to caspase cascade-regulated and mitochondrial-mediated cell death [22,23]. Thus, the significant increased expression level of the *Bad* gene indicates the involvement of mitochondrial proteins in MCP-induced apoptosis and cell injury in hUCBSCs. There are indirect, but important, lines of evidence showing the effect of Akt signaling on cell survival in the maintenance of mitochondrial membrane potential [40,41].

In summary, Akt plays a significant role in the regulation of MCP-induced apoptosis in hUCBSCs. MCP shows strong binding with kinase and the AGC-kinase C-terminal regulatory domain of Pkb/Akt. This interaction impairs the phosphorylation of Pkb/Akt on the Thr309 and Ser473 positions. MCP-induced downregulation of pAkt in hUCBSCs

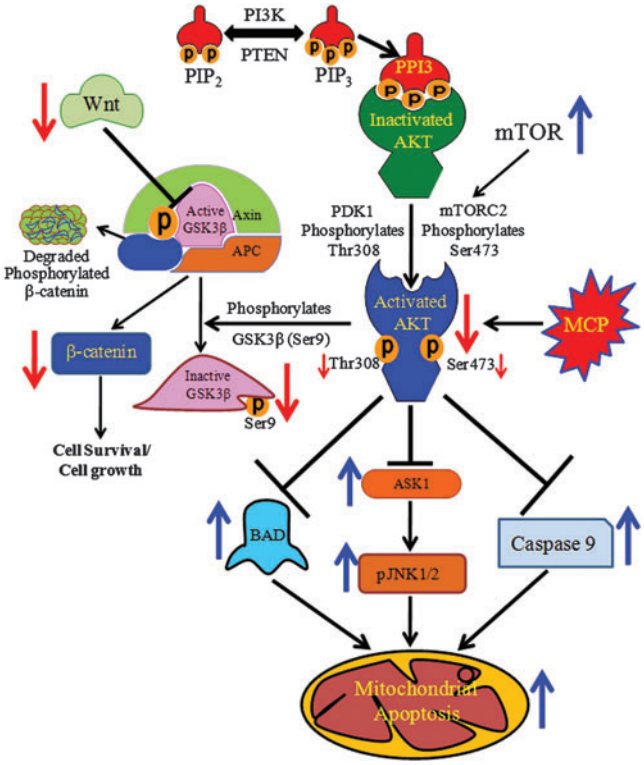

FIG. 9. Schematic flow chart depicting the mechanisms involved in Akt-mediated regulation in MCP-induced apoptosis in cultured human umbilical cord blood stem cells. Color images available online at www.liebertpub.com/scd

was found to be associated with the impaired expression of the Wnt/GSKβ/β-catenin pathways. At the same time, upregulated expression of ASK1/pJNK1/2 and Bad could be associated with upregulated expression of P^{53}, P^{21}, Bax, and activated caspase-9 and 3 (Fig. 9). Our data suggest that the Akt protein plays an important role in MCP-induced apoptosis in hUCBSCs. We also identified that MCP induces the cellular responses through strong binding and inhibition of kinase and the AGC-kinase C-terminal regulatory domain of Akt protein.

Acknowledgments

Authors are grateful to the director, IITR, Lucknow, India, for his keen interest in the study. The work was supported by the Council of Scientific & Industrial Research (CSIR), New Delhi, India, (Grant Supra Institutional Project SIP-08) and the Department of Biotechnology (DBT), New Delhi, India (grant no. 102/IFD/SAN/PR-1524/2010-201). The University Grant Commission (UGC), New Delhi, India, is acknowledged for providing the fellowship to Dr. M.P. Kashyap. The funders had no role in study design, data collection and analysis, decision to publish, or preparation of the article.

Author Disclosure Statement

Authors of this article have no conflicts of interest among them or anybody else regarding the scientific contents, financial matters, and otherwise.

References

1. Shrotriya S, JK Kundu, HK Na and YJ Surh. (2010). Diallyl trisulfide inhibits phorbol ester-induced tumor promotion, activation of AP-1, and expression of COX-2 in mouse skin by blocking JNK and Akt signaling. Cancer Res 70:1932–1940.
2. Shibata M, F Hakuno, D Yamanaka, H Okajima, T Fukushima, T Hasegawa, T Ogata, Y Toyoshima, K Chida, et al. (2010). Paraquat-induced oxidative stress represses phosphatidylinositol 3-kinase activities leading to impaired glucose uptake in 3T3-L1 adipocytes. J Biol Chem 285:20915–20925.
3. Briz V, JM Molina-Molina, S Sanchez-Redondo, MF Fernandez, JO Grimalt, N Olea, E Rodriguez-Farre and C Sunol. (2011). Differential estrogenic effects of the persistent organochlorine pesticides dieldrin, endosulfan, and lindane in primary neuronal cultures. Toxicol Sci 120:413–427.
4. Manning BD and LC Cantley. (2007). AKT/PKB signaling: navigating downstream. Cell 129:1261–1274.
5. Lippa B, G Pan, M Corbett, C Li, GS Kauffman, J Pandit, S Robinson, L Wei, E Kozina, et al. (2008). Synthesis and structure based optimization of novel Akt inhibitors. Bioorg Med Chem Lett 18:3359–3363.
6. Coloff JL, EF Mason, BJ Altman, VA Gerriets, T Liu, AN Nichols, Y Zhao, JA Wofford, SR Jacobs, et al. (2011). Akt requires glucose metabolism to suppress puma expression and prevent apoptosis of leukemic T cells. J Biol Chem 286:5921–5933.
7. Garofalo RS, SJ Orena, K Rafidi, AJ Torchia, JL Stock, AL Hildebrandt, T Coskran, SC Black, DJ Brees, et al. (2003). Severe diabetes, age-dependent loss of adipose tissue, and mild growth deficiency in mice lacking Akt2/PKB beta. J Clin Invest 112:197–208.
8. Yang ZZ, O Tschopp, A Baudry, B Dummler, D Hynx and BA Hemmings. (2004). Physiological functions of protein kinase B/Akt. Biochem Soc Trans 32:350–354.
9. Chung S, J Yao, K Suyama, S Bajaj, X Qian, OD Loudig, EA Eugenin, GR Phillips and RB Hazan. (2012). N-cadherin regulates mammary tumor cell migration through Akt3 suppression. Oncogene [Epub ahead of print]; Doi: 10.1038/onc.2012.65.
10. Stuenaes JT, A Bolling, A Ingvaldsen, C Rommundstad, E Sudar, FC Lin, YC Lai and J Jensen. (2010). Beta-adrenoceptor stimulation potentiates insulin-stimulated PKB phosphorylation in rat cardiomyocytes via cAMP and PKA. Br J Pharmacol 160:116–129.
11. Wu WI, WC Voegtli, HL Sturgis, FP Dizon, GP Vigers and BJ Brandhuber. (2010). Crystal structure of human AKT1 with an allosteric inhibitor reveals a new mode of kinase inhibition. PLoS One 5:e12913.
12. Kumar CC and V Madison. (2005). AKT crystal structure and AKT-specific inhibitors. Oncogene 24:7493–7501.
13. Lindsley CW, SF Barnett, M Yaroschak, MT Bilodeau and ME Layton. (2007). Recent progress in the development of ATP-competitive and allosteric Akt kinase inhibitors. Curr Top Med Chem 7:1349–1363.
14. Ranatunga S and JR Del Valle. (2011). Synthesis of GSK3beta mimetic inhibitors of Akt featuring a novel extended dipeptide surrogate. Bioorg Med Chem Lett 21:7166–7169.
15. Zhou HY and SL Huang. (2012). Current development of the second generation of mTOR inhibitors as anticancer agents. Chin J Cancer 31:8–18.
16. Mukherjee B, N Tomimatsu, K Amancherla, CV Camacho, N Pichamoorthy and S Burma. (2012). The dual PI3K/mTOR inhibitor NVP-BEZ235 is a potent inhibitor of ATM- and DNA-PKCs-mediated DNA damage responses. Neoplasia 14:34–43.
17. Barr DB, A Bishop and LL Needham. (2007). Concentrations of xenobiotic chemicals in the maternal-fetal unit. Reprod Toxicol 23:260–266.
18. Zhao M, Y Zhang, C Wang, Z Fu, W Liu and J Gan. (2009). Induction of macrophage apoptosis by an organochlorine insecticide acetofenate. Chem Res Toxicol 22:504–510.
19. Chatterjee S, P Basak, M Chaklader, P Das, JA Pereira, S Chaudhuri and S Law. (2011). Pesticide induced alterations in marrow physiology and depletion of stem and stromal progenitor population: an experimental model to study the toxic effects of pesticide. Environ Toxicol [Epub ahead of print]; Doi: 10.1002/tox.20775.
20. Alexander FE, SL Patheal, A Biondi, S Brandalise, ME Cabrera, LC Chan, Z Chen, G Cimino, JC Cordoba, et al. (2001). Transplacental chemical exposure and risk of infant leukemia with MLL gene fusion. Cancer Res 61:2542–2546.
21. Ma X, PA Buffler, RB Gunier, G Dahl, MT Smith, K Reinier and P Reynolds. (2002). Critical windows of exposure to household pesticides and risk of childhood leukemia. Environ Health Perspect 110:955–960.
22. Kashyap MP, AK Singh, MA Siddiqui, V Kumar, VK Tripathi, VK Khanna, S Yadav, SK Jain and AB Pant. (2010). Caspase cascade regulated mitochondria mediated apoptosis in monocrotophos exposed PC12 cells. Chem Res Toxicol 23:1663–1672.
23. Kashyap MP, AK Singh, V Kumar, VK Tripathi, RK Srivastava, M Agrawal, VK Khanna, S Yadav, SK Jain and AB Pant. (2011). Monocrotophos induced apoptosis in PC12 cells: role of xenobiotic metabolizing cytochrome P450s. PLoS One 6:e17757.
24. Kalani K, DK Yadav, F Khan, SK Srivastava and N Suri. (2012). Pharmacophore, QSAR, and ADME based semi-synthesis and in vitro evaluation of ursolic acid analogs for anticancer activity. J Mol Model 18:3389–3413.
25. Jain AN. (2007). Surflex-Dock 2.1: robust performance from ligand energetic modeling, ring flexibility, and knowledge-based search. J Comput Aided Mol Des 21:281–306.
26. Pan J, GY Liu, J Cheng, XJ Chen and XL Ju. (2010). CoMFA and molecular docking studies of benzoxazoles and benzothiazoles as CYP450 1A1 inhibitors. Eur J Med Chem 45:967–972.
27. Sander T, T Liljefors and T Balle. (2008). Prediction of the receptor conformation for iGluR2 agonist binding: QM/MM docking to an extensive conformational ensemble generated using normal mode analysis. J Mol Graph Model 26:1259–1268.
28. Larosa F, E Deconinck, P Helias, J Fontan, M Heczko, A Brion, K Ledu, P Delaby, J Vuiller, et al. (2011). Successful mobilization and engraftment of PBSCs derived from donor cord blood cells after a previous allogeneic RIC single unrelated cord blood transplantation. Blood 118:476–478.
29. Zanier ER, M Montinaro, M Vigano, P Villa, S Fumagalli, F Pischiutta, L Longhi, ML Leoni, P Rebulla, et al. (2011). Human umbilical cord blood mesenchymal stem cells protect mice brain after trauma. Crit Care Med 39:2501–2510.
30. Gluckman E, HA Broxmeyer, AD Auerbach, HS Friedman, GW Douglas, A Devergie, H Esperou, D Thierry, G Socie, et al. (1989). Hematopoietic reconstitution in a patient with Fanconi's anemia by means of umbilical-cord blood from an HLA-identical sibling. N Engl J Med 321:1174–1178.
31. Kilpatrick DC, AP Atkinson, JB Palmer, WG Murphy and ML Turner. (1998). Developmental variation in stem-cell

markers from human fetal liver and umbilical cord blood leukocytes. Transfus Med 8:103–109.
32. Bornstein R, AI Flores, MA Montalban, MJ del Rey, J de la Serna and F Gilsanz. (2005). A modified cord blood collection method achieves sufficient cell levels for transplantation in most adult patients. Stem Cells 23:324–334.
33. Isoda H, TP Talorete, J Han, S Oka, Y Abe and Y Inamori. (2005). Effects of organophosphorous pesticides used in china on various mammalian cells. Environ Sci 12:9–19.
34. Das GP, AP Shaik and K Jamil. (2006). Estimation of apoptosis and necrosis caused by pesticides in vitro on human lymphocytes using DNA diffusion assay. Drug Chem Toxicol 29:147–156.
35. Sunmonu TO and OB Oloyede. (2010). Performance and haematological indices in rats exposed to monocrotophos contamination. Hum Exp Toxicol 29:845–850.
36. Gurbani D, V Kukshal, J Laubenthal, A Kumar, A Pandey, S Tripathi, A Arora, SK Jain, R Ramachandran, D Anderson and A Dhawan. (2012). Mechanism of inhibition of the ATPase domain of human topoisomerase IIalpha by 1,4-benzoquinone, 1,2-naphthoquinone, 1,4-naphthoquinone, and 9,10-phenanthroquinone. Toxicol Sci 126:372–390.
37. Freeman-Cook KD, C Autry, G Borzillo, D Gordon, E Barbacci-Tobin, V Bernardo, D Briere, T Clark, M Corbett, et al. (2010). Design of selective, ATP-competitive inhibitors of Akt. J Med Chem 53:4615–4622.
38. McManus EJ, K Sakamoto, LJ Armit, L Ronaldson, N Shpiro, R Marquez and DR Alessi. (2005). Role that phosphorylation of GSK3 plays in insulin and Wnt signalling defined by knockin analysis. EMBO J 24:1571–1583.
39. Galluzzi L, K Blomgren and G Kroemer. (2009). Mitochondrial membrane permeabilization in neuronal injury. Nat Rev Neurosci 10:481–494.
40. Plas DR and CB Thompson. (2005). Akt-dependent transformation: there is more to growth than just surviving. Oncogene 24:7435–7442.
41. Robey RB and N Hay. (2006). Mitochondrial hexokinases, novel mediators of the antiapoptotic effects of growth factors and Akt. Oncogene 25:4683–4696.

Address correspondence to:
Dr. Aditya B. Pant
In Vitro Toxicology Laboratory
Indian Institute of Toxicology Research
Council of Scientific & Industrial Research
Post Box 80, MG Marg
Lucknow 226001
India

E-mail: abpant@rediffmail.com; abpant@yahoo.com

Received for publication April 26, 2012
Accepted after revision June 27, 2012
Prepublished on Liebert Instant Online August 16, 2012